DOI: 10.1002/ ((please add manuscript number))
Article type: Full Paper

Decoupling Ionic and Electronic Currents in Melanin

Margarita Sheliakina, Albertus Bernardus Mostert and Paul Meredith**

M. Sheliakina
Centre for Organic Photonics & Electronics, The University of Queensland, St Lucia, QLD 4072, Australia
Dr. A. B. Mostert
Department of Chemistry, Swansea University, Singleton Park, SA2 8PP, Wales, United Kingdom
Prof. P. Meredith
Department of Physics, Swansea University, Singleton Park, SA2 8PP, Wales, United Kingdom
E-mail: a.b.mostert@swansea.ac.uk; paul.meredith@swansea.ac.uk

Keywords: melanin, hydration, ionic, bioelectronics, impedance spectroscopy

Melanin, the human skin pigment, has emerged as a model material for bioelectronic interfaces due to its biocompatibility, ability to be processed into electronic-device-grade thin films, and transducing charge transport properties. These charge transport properties have been suggested to be of a mixed protonic/electronic nature, regulated by a redox reaction that can be manipulated by changing the material's hydration state. However, to date, there are no detailed reports which clarify, quantify or disentangle the protonic and electronic contributions to long-range current conduction in melanin. Described herein, is a systematic hydration controlled electrical study on synthetic melanin thin films utilizing impedance/dielectric spectroscopy, which rationally investigates the protonic and electronic contributions. Through modelling and inspecting the frequency dependent behavior, it is shown that the hydration dependent charge transport is due to proton currents. Results show a real dielectric constant for hydrated melanin of order ~ 1 x 10^3. Surprisingly, this very high value is maintained over a wide frequency range of ~ 20 Hz to 10^4 Hz. The electronic component appears to have little influence on melanin's hydration dependent conductivity: thus the material should be considered a protonic conductor, and not as previously suggested, a mixed protonic/electronic hybrid.

1. Introduction

Electroceuticals, a term recently coined by the British drug company GlaxoSmithKline, is the attempt to "…speak the electrical language of the nerves to achieve higher treatment effect".[1] This specific need has been represented even more broadly by the United States National Academy of Engineering, which has presented the need to "advance health informatics" among its 14 grand challenges for engineering in the 21st century.[2] Thus, the search is on to develop therapeutic and monitoring devices that can interface seamlessly with biological systems, with one aim being to enhance personalised healthcare.[3] This vision is the raison d'être of the field of bioelectronics, a rapidly growing branch of the organic electronics community[4-7] that exists at the boundaries of biology, physics, biotechnology, medicine, advanced materials and electrical engineering.[5,8-10]

Ions are the predominant signal carrying entities in biology, whereas our everyday electronics are based upon electron/holes as the main charge carriers transported through semiconductors and metals. Thus, one of the key challenges explored within bioelectronics is the task of realising efficient communication and signal processing between ionic and electronic currents.[5,10] Broadly speaking we refer to this as transduction.

One material that has emerged as a model transducing interface for bioelectronic devices is the brown-black natural pigment melanin.[11] This material is ubiquitous throughout the biosphere, and plays many important functional roles in higher-and-lower-order organisms including humans.[11,12] There are several reasons why melanin has attracted interest in this regard: i) it is biocompatible;[11] ii) it can be processed to create device-quality thin films;[13-18] and iii) most importantly, it appears to sustain a solid-state protonic current, though with an apparent electronic component.[19-23] This last property has been attributed to a redox reaction, the comproportionation equilibrium[20,22] (**Figure 1**) in which the long-range conductivity is regulated by the local density of protons (associated with hydronium – H_3O^+) and semiquinone (SQ) free radicals. Importantly, the charge density can be modulated by changing the state of

hydration, with the water matrix also acting as the proton transporting medium *via* the Grötthus Mechanism akin to localized hole hopping in a disordered semiconductor.[17,19-23] The reaction in **Figure 1** is a simple manifestation of Le Chatelier's principle with the addition of water driving hydronium and SQ formation, and long range proton transport occurring above a matrix percolation threshold. This process leads to orders of magnitude change in the conductivity of melanin as a function of water content.[19,20,22,24] It is interesting to speculate whether the mechanism is generic amongst other biomacromolecules that support electrical currents such as proteins[25] or polysaccharides[26]. Irrespective of this broader context, a natural question arises in the melanin system: which of the two potential charge carriers (proton or free radical), dominates the current, or are they both significant contributors? Recent work appears to indicate that the protonic current is the dominant component,[21] but there are also multiple reports invoking a substantial electronic element.[27-29] Thus there is a clear need to quantify the relative contributions of protons and electrons to the current, and if possible, decouple their behaviour to define accurate structure-property relationships. This will enable rational materials-and-device-level design to advance bioelectronics.

Currently, there is only one study from the 1970's that attempts to quantify the relative contributions using a coulombmetric approach.[23] This study indicated a relative contribution of 65% protonic current and 35% electronic current – however, the coulombmetric method only captures electrode-sample-surface electrochemical effects and would thus naturally report both current types. Recent advances in bioelectronic device architectures, materials processing, contacting, and experimental measurement techniques mean we can now probe bulk effects in the solid-state and thus address this question in a reliable and systematic manner. To this end, we have employed electrical alternating current (AC)/impedance measurements on device-quality melanin thin films in a planar contact architecture as a function of carefully controlled hydration. The relative transport physics of the two carriers are dominated by the large mass

discrepancy between the proton and electron, and this delivers radically different frequency dependent signatures which we successfully isolate. Finally, we've also used H_2O and D_2O to probe any potential kinetic isotope effect, as was recently reported on cephalopod proteins.[30]

2. Results and Discussion

2.1. Nyquist Modelling

Presented in **Figure 2** are the hydration dependent Nyquist plots (imaginary *versus* real components of the complex impedance) of melanin thin films exposed to an H_2O atmosphere (relative vapour pressure indicated). The data clearly exhibits two basic features to be accounted for: i) a distinct higher frequency (low impedance) semi-circle, which is coupled to ii) a low frequency line or tail (higher impedance regime), though we note the absence of the tail at vacuum, which only shows part of the low impedance semi-circular feature. In **Figure 2** we plot both the linear and logarithmic representations to demonstrate these clear features and their dependence upon hydration of the film. The presence of these two basic features immediately implies that a form of the Randall circuit may be appropriate for analysis.

As such, the relevant Randall circuit employs a Warburg element to capture diffusion of ions for the low frequency regime and generally has an impedance form of $Z(\omega) \propto \omega^{-1/2}$. Such an impedance is characterized by a straight line at an angle of 45° (slope = 1 indicated as the blue dashed lines in the linear-linear plots)[31,32]. It is clear that the slope is > 1 for all data sets, indicating a mass diffusion system with a blocking electrode[31-34]. This is consistent with the architecture employed (Ag top contact, ITO bottom contact) and a dominant proton displacement current. Furthermore, it should also be noted that the low frequency line does not change slope and asymptote to 90° - a feature indicative of an ordinary diffusion process, the absence of which is strongly suggestive of anomalous diffusion, i.e. non-Fickian[32,34].

The data presented in **Figure 2**, characterized as described above by a semicircle in the high-frequency regime and a linear dependence in the low-frequency regime is a known and reported fingerprint of proton conductors contacted by blocking electrodes.[30,35] If electronic

conduction was significant alongside protonic conduction, one would expect two semi-circular features with no linear region.[35]

With these considerations in mind, we modelled the data to the minimal equivalent circuit depicted in **Figure 3**, a modified Randles circuit. The circuit consists of: a resistor, which represents the contact resistance; a constant phase element (CPE – a capacitor with a small real component), which represents the dielectric double layer; a second resistor representing the ionic dissipative current; and a modified restricted diffusion element to capture anomalous mass diffusion at a blocking electrode. We restricted ourselves to these elements to reduce the potential spurious effects from a large number of fitting parameters.

The model captures the high frequency response, especially when the film is hydrated, but fails in the low frequency regime. The model fits are shown as dashed red lines in both linear and logarithmic representations. It is clear that the low frequency data does not exhibit a uniform slope as a function of frequency. As far as we are aware, no diffusion circuit element is currently able to capture a changing gradient diffusion tail. Hence, we believe this circuit is a reasonable, simple model that captures the essence of the material behaviour in relation to ion diffusion. We also note, as one would expect, that the dry films show no low frequency tail since according to **Figure 1** there will be a low concentration of free protons. However, for consistency we applied the same equivalent circuit to all hydrations.

The first clear conclusion that can be drawn from the above is that this circuit represents ionic conduction behaviour only, albeit with anomalous (non-Fickian) behaviour. There is no electronic component included in the model, nor indeed did our attempts to include one lead to any reasonable fit to the experimental data. We would emphasise that this analysis is contra to our previous suppositions that melanin may be a mixed electronic/ionic conductor,[19,20] albeit with a proton displacement current dominating the DC response. Hence, the hybrid electronic/protonic model was thoroughly and rigorously tested.

To confirm that the AC modelling parameters extracted from our thin films measurements agree with previously published DC conductivity (and related muon spin relaxation) findings, we plotted the ion dissipative current resistance (R_2) *versus* relative pressure. We would expect that R_2 would decrease with hydration if our impedance measurements were in line with these previous observations. Inspecting **Figure 4** it can be clearly seen that the resistance does indeed decrease exponentially with hydration by ~ 5 orders of magnitude (dry to wet). This indicates that the ionic current is increasing exponentially, which based upon previous work, is in line with an exponential increase in the proton density. This is a strong correlatory evidence.

Finally, comparing the relative effects of H_2O and D_2O (**Figure S1**), we do not observe measurable differences in behaviour. This is in contrast to previous work where we did see differences between H_2O and D_2O in the DC conductivities of pressed melanin powder pellets over mm-length-scales.[22] Furthermore, other related work on cephalopod proteins[30] has indicated a kinetic isotope effect. However, the AC measurements under consideration in this current work were performed on thin films with much narrower electrode gaps (of order 70 nm, i.e. the film thickness). Kinetic isotope effects are very subtle when manifest in bulk electrical measurements, and as such we are simply not sensitive to them in our thin film configuration.

2.3. Ionic Conductivity

In order to estimate the ionic conductivity, it is useful to first present the dielectric responses ε (both the real and imaginary components) *versus* frequency (Bode plots) – we do so for both D_2O and H_2O hydration in **Figure 5**.[36] Surprisingly, for the hydrated samples, the real component of ε is high ($0.5 – 1.0 \times 10^3$) across a wide frequency range ($20 – 10^4$ Hz). This observation is consistent with recent reports of melanin being used as a battery storage medium,[37] but nonetheless is an important and intriguing outcome of the these dielectric measurements.

Using the data presented in **Figure 5**, the ionic conductivity can be estimated by observing that ionic currents dominate at low frequency. Hence, one can use the simple relationship $\varepsilon'' \sim \sigma/\omega$ for the low frequency regime, where σ is the conductivity (ionic) and ω is the radial frequency.[36] However, it is important to note that there may be two competing effects at low hydration, the ion current, but also electrode polarization effects.[36] A signature feature for the latter is if a secondary step increase can be observed in ε' with a concomitant increase in ε'' at low frequencies (typically around 10^{-2} Hz).[36] We do not observe such features in our data, confirming that the low frequency behaviour in **Figure 5** (and indeed **Figure 2**) is due to ions. Further, we note that in the limit where the measured frequency is less than the characteristic frequency of the diffusion element, $\omega_d > \omega$, the diffusion element is given by $Z(\omega) = \frac{1}{3}R_d + R_d(\omega_d/i\omega)^{\gamma}$, i.e. a resistor in series with a constant phase element[32]. This observation means that data below ω_d has to account not only for the dissipative resistor R_2 but also R_d, hence providing another reason to determine the true conductivity of the films from the low frequency region of the Bode plots.

Based upon this rationale, conductivities were extracted from **Figure 5** based upon a frequency range of 20-60 Hz, which are plotted in **Figure 6**. The data is striking in several respects – in particular a 3 orders of magnitude change is observed over the hydration range of 0 mbar to 20 mbar (both H_2O and D_2O data sets, note that **Figure 6** is normalized to relative pressure). This is significantly larger than reported for pressed powder samples,[19,20,22] which is not so surprising given the radically different morphologies. It is also important to qualify that the changes in film thickness with hydration have been appropriately normalised using recently published Neutron Reflectometry data of hydrated melanin thin films[38]. Thus, the large changes in conductivity are not due to thickness changes on the measured samples, and furthermore are consistent with the equivalent circuit modelling presented in **Figure 4**. It is therefore very likely that the large changes in electrical conductivity in multiple sample types

and measurement configurations[17,19-23,39] reported in the literature essentially captured ionic rather than mixed ionic/electronic currents.

Finally, in light of the above observations, we can approximately determine the proton charge density in our melanin thin films at high hydration levels. Assuming that the mobility of the protons is determined by the Grötthus mechanism for hydrated bioelectronic materials,[40] i.e. $\mu \sim 10^{-3}$ $cm^2V^{-1}s^{-1}$, then a respectable proton charge density of $n \sim 10^{19}$ cm^{-3} is obtained from the simple conductivity relation.

3. Conclusion

In conclusion, using hydration controlled impedance measurements we have probed the nature of the dominant charge carrier in solid-state melanin thin films. We observe a systematic growth in the low frequency response as hydration increases for both D_2O and H_2O adsorption. The high frequency component appears invariant. This is strongly suggestive of the main component of the current being ionic or more precisely protonic. We have developed a minimal equivalent circuit to describe this behaviour, the salient features of which are a constant phase element and resistor representing the ionic displacement current with a modified restricted diffusion element in series. All the Nyquist impedance plots fit this circuit, and no combination of elements delivers a significant electronic component. The modelling therefore confirms the dominant current component to be protonic. Determination of the dielectric constant (real and imaginary parts) allow the ionic conductivity to be estimated. As per previous literature we observe significant changes dry-to-wet of ~3 orders of magnitude. An unexpected and interesting finding from these measurements is the high real part of the dielectric constant (~10^3) over a wide frequency range (20 to 10^4 Hz). Finally, assuming a Grötthus–like mobility, we estimate the proton charge density to be ~ 10^{19} cm^{-3}. Our findings are significant since they strongly indicate that melanin is not a mixed hybrid electronic-ionic conductor as previously thought – but a proton transport material.

4. Experimental Section

Materials: Melanin was synthesized following a standard literature procedure,[41,42] utilizing as the initial starting material D,L-dopa (Sigma-Aldrich). D,L-dopa was dissolved in deionized water, subsequently adjusted to pH 8 using NH_3 (28%). Air was then bubbled through the solution while being stirred for 3 days. The solution was then brought to pH 2 using HCl (32%) to precipitate the pigment. The solution was then filtered and washed multiple times with deionized water and dried. The obtained powder was used to make a solution for thin film fabrication according to previous published work.[13] In brief, the solution composition was ~0.7 g melanin in 5 ml H_2O and 10 ml NH_3 (28%), which was stirred for 1 hour at room temperature and then ultra-sonicated for 1 hour.

Device Fabrication: Glass slides (15 mm x 15 mm) with 80 nm thick patterned ITO were cleaned with Alcanox, rinsed in water and ultra-sonicated in acetone (5 min). Afterwards they were rinsed with deionized water, ultra-sonicated in 2-propanol (5 min) and dried under a flow of nitrogen. The substrates were finally treated with UV-Ozone (20 min). A thin film of melanin was spin coated at 500 rpm for 5 sec followed by 1500 rpm for 60 s. Film thicknesses of 70 nm were obtained as measured using a DEKTAK profilometer. Finally 30 nm Ag top electrodes were thermally evaporated on top of the melanin films.

Electrical Measurements: Hydration dependent experiments were performed using a vacuum capable chamber[19,20] and utilising an Angilent E4980A LCR meter, taking measurements from 20Hz to 1MHz. In order to have confidence in our measurements, we had to satisfy two criteria: 1) that our samples were at equilibrium with the hydrating environment; 2) that our measurements did not have capacitances dominating from the measurement line. The latter issue occurs when a planar geometry is utilised in AC measurements (as used elsewhere[21]) on thin films of material. Essentially, the electrode surface area is minimal and thus the capacitance of the sample is less than that of the electrical wiring. To overcome these contradictory requirements, we developed a liquid contact setup in which the melanin thin film

was brought into temporary contact to a metal liquid electrode (EGaIn, (Sigma-Aldrich)), which then could be disconnected to expose the film to the environment.

We then compared these results to samples which had pre-evaporated top contacts (see Device Fabrication above), which presumably could retard equilibration with the environment. Our results showed that the dependencies on hydration were similar with pressures up to 15 mbar (see **Figure S2**), which indicated that standard devices did come into equilibrium with the environment in spite of the top electrode.

Hydrating Atmosphere: The chamber was pumped down to vacuum for 2 hours using a rotary pump. Desired water pressures (5 mbar increments) were achieved by isolating the pump and bleeding in water vapour (Milli-Q, freeze-thaw-pumped 3 times) to a specific pressure read using a BOC-Edwards GK series (0-50mbar) gauge. The same procedure was used for D_2O. Each pressure was held for an hour to insure equilibrium was reached in line with previously published work and noting the equilibration concerns described above.[38] All absolute pressures were then normalised to a relative pressure value, using a room temperature saturation pressure of 24 mbar for H_2O, and 20 mbar for D_2O.

Modelling: Modelling was undertaken utilizing the EC-lab software (Demonstration Version). The minimum number of equivalent circuit parameters were selected that gave a reasonable fit to the impedance plots. Data was then also normalized to yield the dielectric response by taking into account the thickness of the film, while accounting for any thickness changes due to swelling in the hydrated atmosphere, as quantified by a previously published Neutron Reflectometry study.[38]

Conductivity Data Analysis: The low frequency data for the imaginary component of the dielectric spectra is proportional to $\sim\sigma/\omega$. The data was linearized over a frequency range of 20-60 Hz for all curves and the conductivity extracted *via* least square fitting. Uncertainties

were determined based upon 2 times standard error from the fits. The frequency ranges were selected such that the data was linear and captured the ionic processes.

Supporting Information
Supporting Information is available from the Wiley Online Library or from the authors.

Acknowledgements
PM is a Sêr Cymru Research Chair, an Honorary Professor at the University of Queensland, and formerly an ARC Discovery Outstanding Researcher Award Fellow. This work was supported by the Australian Research Council through its Discovery Program (DP140103653) and the Welsh European Funding Office (European Regional Development Fund) through the Sêr Cymru II Program. MS is supported by a University of Queensland International Postgraduate Research Scholarship, and ABM is a Sêr Cymru II fellow and results incorporated in this work have received funding from the European Union's Horizon 2020 research and innovation program under the Marie Skłodowska-Curie grant agreement No 663830. This work was performed in part at the Queensland node of the Australian National Fabrication Facility (ANFF-Q), a company established under the National Collaborative Research Infrastructure Strategy to provide nano- and microfabrication facilities for Australian researchers. We acknowledge funding from the University of Queensland (Strategic Initiative, Centre for Organic Photonics & Electronics). We thank Dr. Ardalan Armin for discussion regarding interpretation.

Received: ((will be filled in by the editorial staff))
Revised: ((will be filled in by the editorial staff))
Published online: ((will be filled in by the editorial staff))

References

[1] S. K. Moore, in *IEEE Spectrum*, Vol. 52, **2015**, 78.
[2] N. A. o. Engineering, in *Grand Challenges for Engineering: Imperatives, Prospects, and Priorities.*, (Ed: N. A. o. Engineering), National Academies Press., Washington **2016**.
[3] J. Andreu-Perez, D. R. Leff, H. M. D. Ip, G. Z. Yang, *IEEE Transactions on Biomedical Engineering* **2015**, 62, 2750.
[4] J. Rivnay, R. M. Owens, G. G. Malliaras, *Chemistry of Materials* **2014**, 26, 679.
[5] P. Meredith, C. J. Bettinger, M. Irimia-Vladu, A. B. Mostert, P. E. Schwenn, *Reports on Progress in Physics* **2013**, 76, 034501.
[6] G. Tarabella, F. M. Mohammadi, N. Copped, F. Barbero, S. Iannotta, C. Santato, F. Cicoira, *Chemical Science* **2013**, 4, 1395.
[7] K. Svennersten, K. C. Larsson, M. Berggren, A. Richter-Dahlfors, *Biochimica Biophysica Acta - General Subjects* **2011**, 1810, 276.
[8] M. Muskovich, C. J. Bettinger, *Advanced Healthcare Materials* **2012**, 1, 248.
[9] M. Irimia-Vladu, *Chemical Society Reviews* **2014**, 43, 588.
[10] R. M. Owens, G. G. Malliaras, *MRS Bulletin* **2010**, 35, 449.
[11] P. Meredith, T. Sarna, *Pigment Cell Research* **2006**, 19, 572.
[12] G. Prota, *Melanins and melanogenesis*, Academic Press, San Diego CA **1992**.
[13] J. Bothma, J. de Boor, U. Divakar, P. Schwenn, P. Meredith, *Advanced Materials* **2008**, 20, 3539.

[14] M. Abbas, F. D'Amico, L. Morresi, N. Pinto, M. Ficcadenti, R. Natali, L. Ottaviano, M. Passacantando, M. Cuccioloni, M. Angeletti, R. Gunnella, *European Physical Journal E* **2009**, 28, 285.
[15] H. Lee, S. M. Dellatore, W. M. Miller, P. B. Messersmith, *Science* **2007**, 318, 426.
[16] M. Ambrico, P. F. Ambrico, A. Cardone, T. Ligonzo, S. R. Cicco, R. Di Mundo, V. Augelli, G. M. Farinola, *Advanced Materials* **2011**, 23, 3332.
[17] J. Wünsche, F. Cicoira, C. F. O. Graeff, C. Santato, *Journal of Materials Chemistry B* **2013**, 1, 3836.
[18] M. P. da Silva, J. C. Fernandes, N. B. de Figueredo, M. Mulato, C. F. O. Graeff, *AIP Advances* **2014**, 4, 037120.
[19] A. B. Mostert, B. J. Powell, I. R. Gentle, P. Meredith, *Applied Physics Letters* **2012**, 100, 093701.
[20] A. B. Mostert, B. J. Powell, F. L. Pratt, G. R. Hanson, T. Sarna, I. R. Gentle, P. Meredith, *Proceedings of the National Academy of Sciences USA* **2012**, 109, 8943.
[21] J. Wünsche, Y. Deng, P. Kumar, E. Di Mauro, E. Josberger, J. Sayago, A. Pezzella, F. Soavi, F. Cicoira, M. Rolandi, C. Santanto, *Chemistry of Materials* **2015**, 27, 436.
[22] S. B. Rienecker, A. B. Mostert, G. Schenk, G. R. Hanson, P. Meredith, *Journal of Physical Chemistry B* **2015**, 119, 14994.
[23] M. R. Powell, B. Rosenberg, *Bioenergetics* **1970**, 1, 493.
[24] T. F. Wu, B. H. Wee, J. D. Hong, *Advanced Materials Interfaces* **2015**, 2, 1500203.
[25] N. Amdursky, X. Wang, P. Meredith, D. D. C. Bradley, M. M. Stevens, *Advanced Materials* **2016**, 28, 2692.
[26] C. Zhong, Y. Deng, A. F. Roudsari, A. Kapetanovic, M. P. Anantram, M. Rolandi, *Nature Communications* **2011**, 2, 476.
[27] E. J. Son, J. H. Kim, K. Kim, C. B. Park, *Journal of Material Chemistry A* **2016**, 4, 11179.
[28] N. F. D. Vecchia, R. Marega, M. Ambrico, M. Iacomino, R. Micillo, A. Napolitano, D. Bonifazi, M. d'Ischia, *Journal of Materials Chemistry C* **2015**, 3, 6525.
[29] G. Tarabella, A. Pezzella, A. Romeo, P. D'Angelo, N. Coppede, M. Calicchio, M. d'Ischia, R. Mosca, S. Iannotta, *Journal of Materials Chemistry B* **2013**, 1, 3843.
[30] D. D. Ordinario, L. Phan, W. G. Walkup IV, J.-M. Jocson, E. Karshalev, N. Husken, A. A. Gorodetsky, *Nature Chemistry* **2014**, 6, 596.
[31] J. Bisquert, G. Garcia-Belmonte, P. Bueno, E. Longo, L. O. S. Bulhoes, *Journal of Electroanalytical Chemistry* **1998**, 452, 229.
[32] J. Bisquert, A. Compte, *Journal of Electroanalytical Chemistry* **2001**, 499, 112.
[33] J. Bisquert, G. Garcia-Belmonte, F. Fabregat-Santiago, P. R. Bueno, *Journal of Electroanalytical Chemistry* **1999**, 475, 152.
[34] J. Bisquert, G. Garcia-Belmonte, A. Pitarch, ChemPhysChem **2003**, 4, 287.
[35] R. A. Huggins, *Ionics* **2002**, 8, 300.
[36] G. Floudas, in *Polymer Science: A Comprehensive Reference*, Vol. 2, Elsevier B.V., **2012**, 825.
[37] Y. J. Kim, W. Wu, S. Chun, J. F. Whitacre, C. J. Bettinger, *Proceedings of the National Academy of Sciences USA* **2013**, 110, 20912.
[38] A. J. Clulow, A. B. Mostert, M. Sheliakina, A. Nelson, N. Booth, P. L. Burn, I. R. Gentle, P. Meredith, *Soft Matter* **2017**, 13, 3954.
[39] M. Jastrzebska, H. Isotalo, J. Paloheimo, H. Stubb, *Journal of Biomaterials Science Polymer Ed.* **1995**, 7, 577.
[40] T. Miyake, M. Rolandi, *Journal of Physics: Condensed Matter* **2016**, 28, 023001.
[41] A. B. Mostert, K. J. P. Davy, J. L. Ruggles, B. J. Powell, I. R. Gentle, P. Meredith, *Langmuir* **2010**, 26, 412.

[42] C. C. Felix, J. S. Hyde, T. Sarna, R. C. Sealy, *Journal of the American Chemical Society* **1978**, 100, 3922.

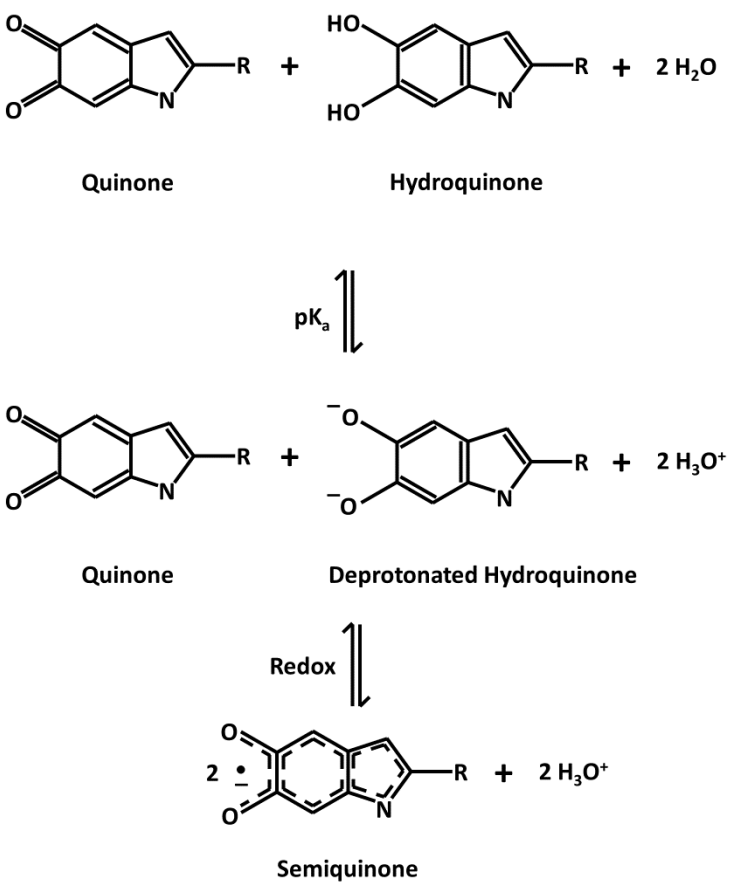

Figure 1. The comproportionation equilibrium reaction which involves two steps: hydroquinone deprotonates which leads to hydronium formation; and the hydroquinone reacts with a quinone in a 1 electron redox reaction to form semiquinone radicals, a moiety of an intermediate oxidative state.

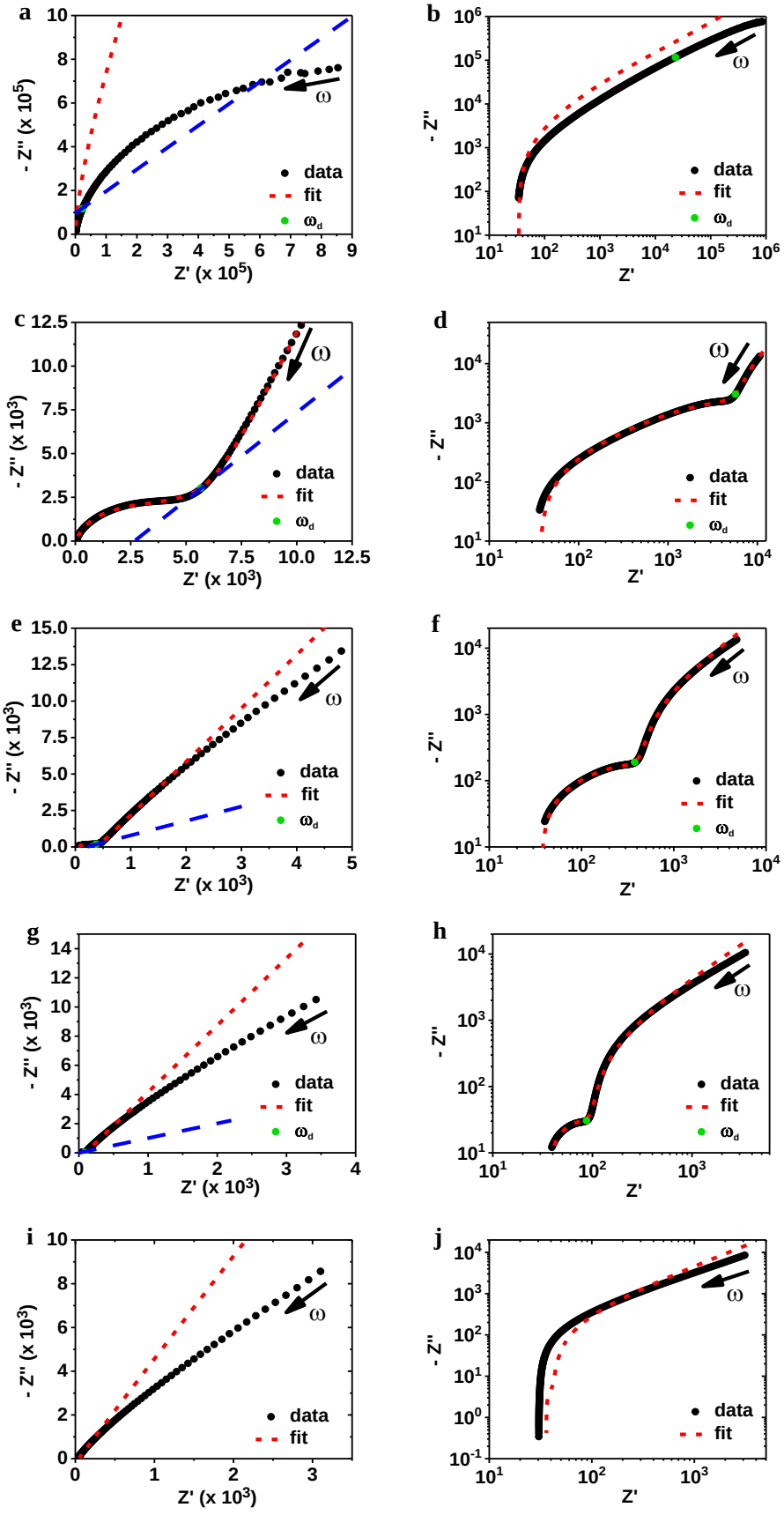
a
- Z'' (x 10^5)
Z' (x 10^5)
ω
data
fit
ω_d
b
- Z''
Z'
c
- Z'' (x 10^3)
Z' (x 10^3)
d
e
f
g
h
i
j

Figure 2. Nyquist plots obtained for a melanin thin film exposed to H_2O. Left column is the data represented on a linear scale, from top to bottom are relative pressures (RP) 0, 0.21, 0.42, 0.63 and 0.83 respectively. The right column is same data but in a log-log plot to show the strength of the fit and accentuate the high frequency features. The minimalist equivalent circuit modelling fits are shown as a red dashed line. Also indicated are lines set at 45° (blue dotted line, left column) and the characteristic frequency ω_d (large green dot) of the diffusion element. Direction of increasing frequency indicated by an arrow.

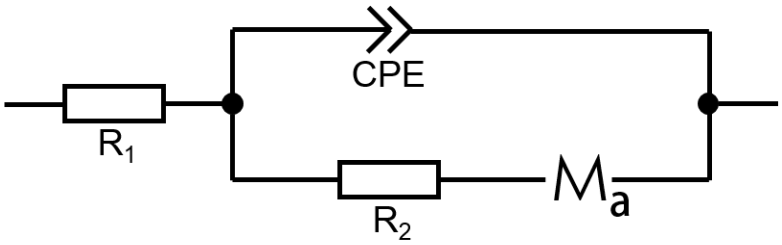

Figure 3. The equivalent circuit used to model our impedance data (Nyquist plots). It includes a contact resistance (R_1), a constant phase element (CPE), an ionic displacement resistance (R_2) and a modified restricted diffusion element (M_a). The equations that describe each element's behavior are provided in the Supplementary Information.

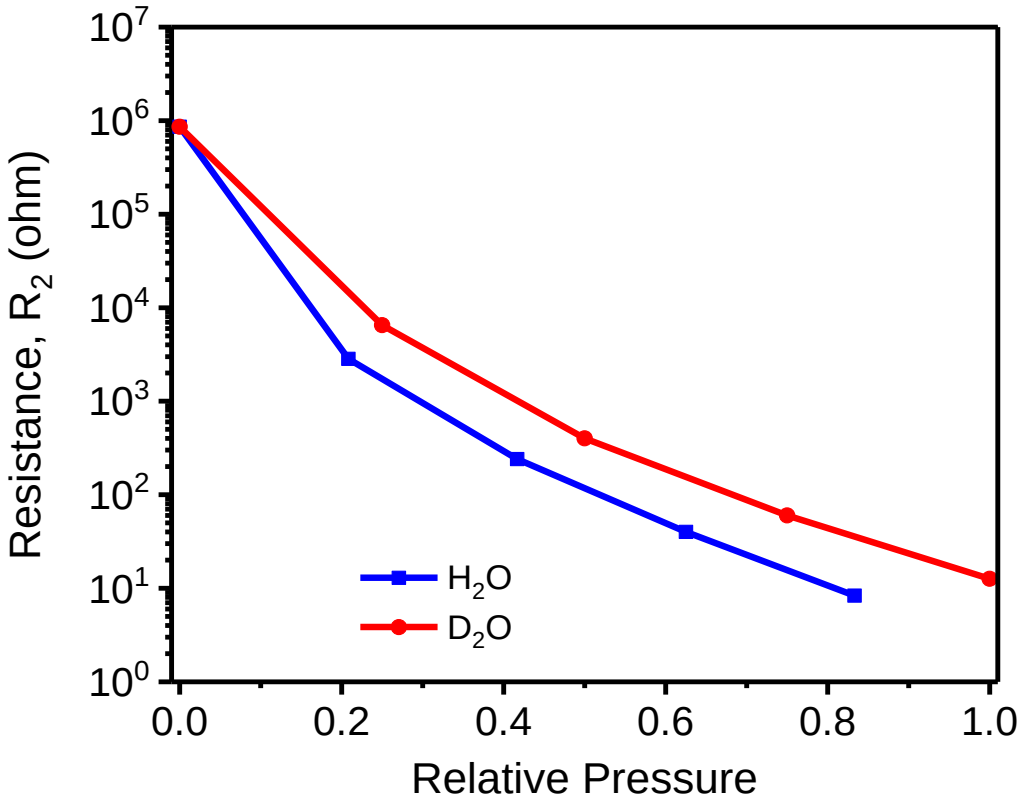

Figure 4. The modelled dissipative current resistance (R_2) as a function of hydration of melanin thin films. The type of water is indicated in the legend.

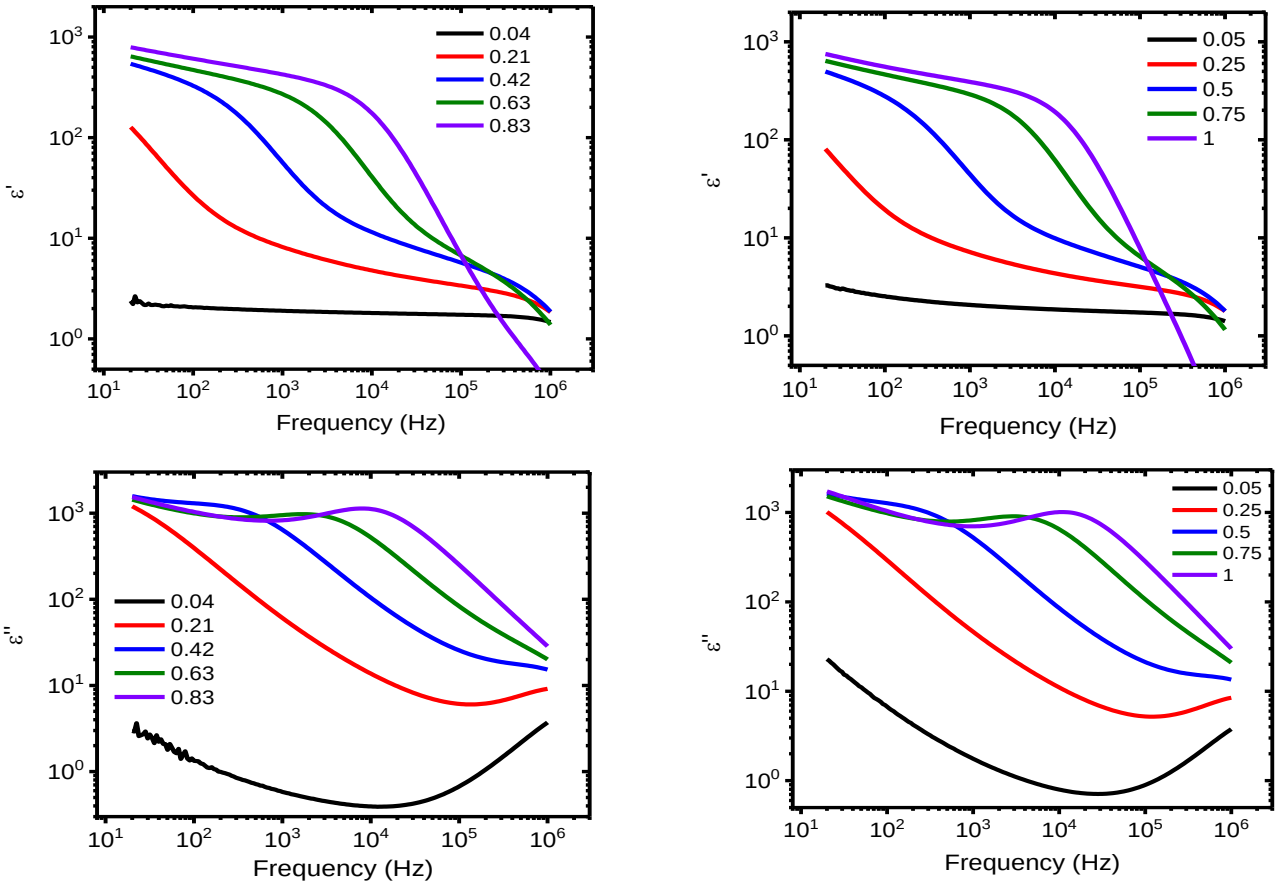

Figure 5. (Top) Real component of the dielectric response *versus* frequency plots for melanin thin films exposed to H_2O (left) and D_2O (right).The imaginary component of the dielectric response can also be seen (bottom data set). The relative pressure is indicated in the legend.

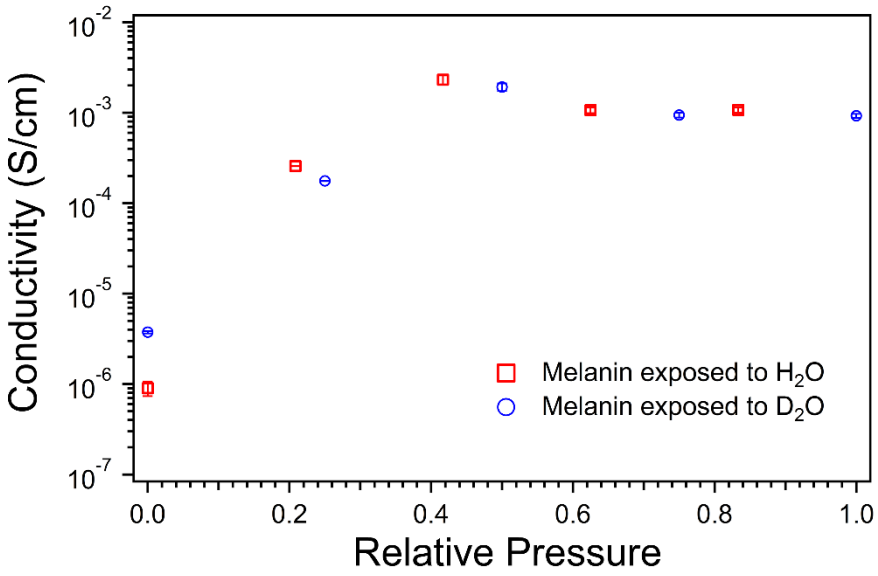

Figure 6. The low frequency conductivity of melanin thin films as a function of relative pressure for both H_2O and D_2O. Conductivity data points were determined within a frequency range of 20-60 Hz.